Bad-Cavity Raman Laser Based on Lattice-Trapped Cesium Atoms

Peng Yu[1,2] Liu Pengfei[3] Li Wei[4]

[1]*School of Science, Beijing Forestry University, Beijing* 100083, *China*

[2]*Institute for Interdisciplinary Information Sciences, Tsinghua University, Beijing* 100084, *China*

[3]*School of Physics, Beijing Institute of Technology, Beijing* 100081, *China*

[4]*China South Industries Institute, Beijing* 100089, *China*

Abstract We propose a bad-cavity laser based on the Raman transition of cesium-133 atoms that collectively emit photons into the wide mode of a low finesse resonator, which is known as the optical bad-cavity regime. The spin-spin correlation, which characterizes the collective effect, is demonstrated. We theoretically predict that the optical radiation has an extremely narrow linewidth in the 98×10^{-2} mHz range, and that a power level of 7×10^{-10} W is possible.

Key words lasers; bad-cavity Raman laser technique; spin-spin correlation; narrow linewidth; collective effect

OCIS codes 140.3320; 020.1335; 020.3320; 020.7010; 140.3460

基于铯原子的坏腔拉曼激光器研究

彭 瑜[1,2] 刘鹏飞[3] 李 伟[4]

[1]北京林业大学理学院, 北京 100083

[2]清华大学交叉信息研究院, 北京 100084

[3]北京理工大学物理学院, 北京 100081

[4]中国南方工业研究院, 北京 100089

摘要 提出一种基于铯原子拉曼跃迁的坏腔激光器。该激光器基于低精细度的共振腔和集体效应来构建光学坏腔模型。通过研究激光线宽理论,得到影响窄线宽激光的几个要素,进而分析实现窄线宽的途径,并使用自旋-自旋相关系数表征集体效应。根据一系列理论分析,发现基于铯原子的坏腔拉曼激光器可实现98×10^{-2} mHz的激光线宽和7×10^{-10} W的激光功率输出。

关键词 激光器; 坏腔拉曼激光技术; 自旋相关; 窄线宽; 集体效应

中图分类号 TN248.1 **文献标识码** A

doi: 10.3788/LOP53.041402

1 Introduction

Narrow-linewidth lasers are highly desirable for applications such as optical atomic clockwork[1-2], gravitational wave detection, cavity quantum electrodynamics[3], quantum optomechanics[4], and precision tests of relativity[5]. The optimal spectral purity of a laser is achieved by using an external optical resonator, *i.e.* an arrangement of two highly reflective mirrors that allows light to reflect back and forth between them many times. The laser linewidth is limited to 125 mHz because of the integrated phase drift, which is induced by the vibration of the cavity mirrors due to thermal noise that cannot be eliminated[6-7].

Recent research indicates that a laser using the ultra-narrow optical transition of atoms in an active optical clock[8-11] configuration can produce far purer spectra, the linewidth of which can be 2 orders of magnitude narrower than that of lasers in the traditional laser regime. The collective atomic dipoles can

收稿日期: 2015-10-20; **收到修改稿日期**: 2015-11-28; **网络出版日期**: 2016-03-30

基金项目: 中央高校基本科研业务费专项资金(BLX2015-09)、国家自然科学基金(11504022)、国家自然科学基金重点项目(31530084)

作者简介: 彭 瑜(1981—),男,博士,讲师,主要从事激光、冷原子、量子存储、光子晶体等方面的研究。

E-mail: pengyu@mail.tsinghua.edu.cn

be isolated from the external environment by a factor of about 10000 when operated with a low intracavity photon number. The output light features a frequency linewidth only 1/10000 of the quantum linewidth limit usually applied to lasers operating in the good-cavity regime. The optical radiation of the active optical clock in the bad-cavity configuration has an extremely narrow linewidth[10-19].

Here, we propose a bad-cavity laser in which more than 1000000 cesium-133 atomic dipoles are synchronized by 20 photons on average in the optical bad-cavity regime, and theoretically predict that the optical radiation has an extremely narrow quantum linewidth limit in the 98×10^{-2} mHz range. A power level of 7×10^{-10} W is achieved in our cesium-133 atomic dipole model, which is higher than those for rubidium-87 and calcium-40.

2 Bad-cavity Raman laser theory

The bad-cavity laser source in which the collective synchronization of nearly 1000000 cesium-133 atomic dipoles is continuously sustained by an average of 20 photons inside the optical cavity is shown in Fig. 1(a). The coherence is stored by the collective effect, and the intra-cavity photons extract phase information at a suitable rate. Thus, the amplitude and phase are mostly stored in the atomic medium, and the laser frequency depends only very weakly on the distance between the mirrors. The pink and yellow balls represent photons and atoms, respectively. A portion of the atomic dipoles in the gain medium achieves synchronization under the influence of the weak intracavity light field.

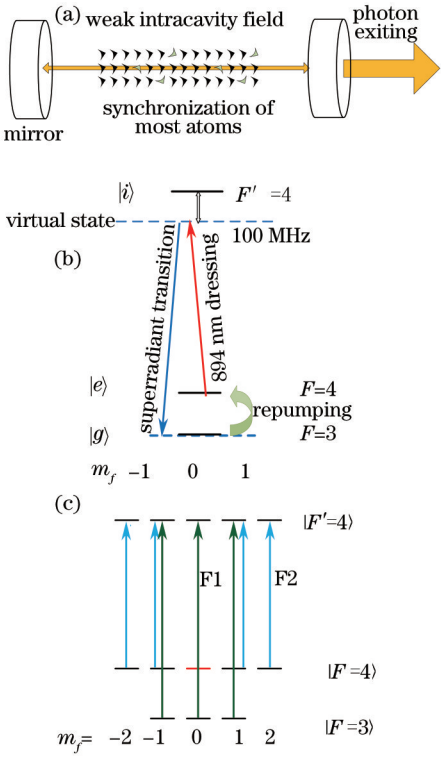

Fig.1 (a) Diagram of bad-cavity cesium laser; (b) two-photon Raman transition of cesium atoms; (c) repumping transitions

Two-photon processes have become a standard tool in atomic physics for exciting atoms to states whose energies are too high to achieve with a single photon and states of the same parity that would normally be inaccessible. Numerous ultrahigh-resolution spectroscopic techniques are based on two-photon processes. We consider the two-photon Raman transition process as a model system, as shown in Fig. 1(b). The metastable ground state $|e\rangle$ is irradiated by a dressing laser (red line) to induce a spontaneous two-photon Raman transition to $|g\rangle$ (blue line), with a tunable transition rate of γ_{eg}. A repumping laser moves atoms from the state $|g\rangle$ back to $|e\rangle$ at a proper rate and thus forms a circle. In

this case, the effective ground state $|e\rangle = |6^2S_{1/2}, \mathrm{F}=4, m_f = 0\rangle$ and the ground state $|g\rangle = |6^2S_{1/2}, F=3, m_f = 0\rangle$ are hyperfine states that are insensitive to magnetic fields. The difference in the frequency between $|e\rangle$ and $|g\rangle$ is only 9.19 GHz. We impose a two-photon stimulated Raman decay from $|e\rangle$ to $|g\rangle$ by applying a linearly polarized 894.6 nm dressing laser tuned 100 MHz lower than the intermediate state $|i\rangle$, $|i\pm\rangle = |6^2P_{1/2}, F' = 4, F'=4, m_f' = \pm 1\rangle$. The transition $|e\rangle \rightarrow |i\rangle$ occurs by the absorption of a photon at the frequency ω_1, and the $|i\rangle \rightarrow |e\rangle$ transition occurs by the emission of a photon at the frequency ω_2. The frequencies are related by $\omega_2 = \omega_1 + \omega_{eg}$. We then obtain the transition probability $W_{e\rightarrow g}$ according to the references [12-13] as follows:

$$W_{e\rightarrow g} = \left|H_{gi,2}\right|^2 \left|H_{ie,1}\right|^2 \sin^2(\omega_0 - \omega_1 + \omega_2)t \Big/ \left[\left(4\hbar^2\right)^2 (\omega_1 - \omega_{ie})^2 (\omega_0 - \omega_1 + \omega_2)^2 / 8\right]. \tag{1}$$

Denoting the detuning of the intermediate state by $\Delta = \omega_1 - \omega_{ie}$, more details are displayed in references [12- 13]. With a dressing pump light, cesium atom transition from $|e\rangle = |6^2S_{1/2}, F=4, m_f = 0\rangle$ through intermediate states $|i\pm\rangle = |6^2P_{1/2}, F' = 4, m_f' = \pm 1\rangle$ to $|g\rangle = |6^2S_{1/2}, F=3, m_f = 0\rangle$ of the transmit path. The intermediate state to the ground state of atomic transition probability is 2.86×10^7 s^{-1}, which is slightly smaller than that of rubidium atoms, 3.6×10^7 s^{-1}. Thus, we design the virtual state near $|i\rangle$ with $\Delta = \omega_1 - \omega_{ie} = 100$ MHz, which will be helpful for determining the transition probability according to Eq. (1).

The dressing laser is typically tuned to 100 MHz to the blue line of the $|e\rangle \rightarrow |i\pm\rangle$ atomic transition. There, pumping lasers are polarized and tuned to the frequency between the ground states and the optical excited state $|6^2P_{3/2}, F' = 4\rangle$ such that the single state dark to the repumping is $|e\rangle$. The F1 repumper moves atoms primarily from the ground $|F = 3\rangle$ state to the ground $|F' = 4\rangle$ state, and the F2 repumper pushes the population to $|e\rangle$, as the Clebsch-Gordan coefficient for the transition $|6^2S_{1/2}, F' = 4, m_f' = 0\rangle \rightarrow |6^2P_{3/2}, F' = 4, m_f' = 0\rangle$ is zero, as shown in Fig. 1(c). The energy-level diagram for the repumping beam shows F2 (blue) and F1 (green). The repumping dark state is labeled with a red line. The single-particle decay rate γ_{eg}, from $|e\rangle$ to $|g\rangle$ is induced by exerting both the repumping and dressing laser. We use an 852.3-nm light to repump atoms from $|g\rangle$ back to $|e\rangle$ at a proper rate w proportional to the total equivalent decay rate to complete the whole circulation.

To understand the role of the collective effect, according to reference [18], we have the equation

$$0 = \left\langle \hat{\sigma}_1^+ \hat{\sigma}_2^- \right\rangle_C \left[-\left(\gamma + w + \frac{2}{T_2}\right)\right] + (w - \gamma) N\gamma C / (w + \gamma) - 2(N\gamma C)^2 \Big/ (\gamma + w) \left\langle \hat{\sigma}_1^+ \hat{\sigma}_2^- \right\rangle_C, \tag{2}$$

where $\Gamma = \gamma + w + 2/T_2$ is the total decay rate of the atomic dipoles. The equation is formulated according to the quantum model of the system and a physically stable solution. The laser threshold is the repumping rate at which the gain $(w-\gamma)N\gamma C/(w+\gamma)$ overcomes the loss Γ. In the limit $\Gamma/N\gamma C \rightarrow 0$, this

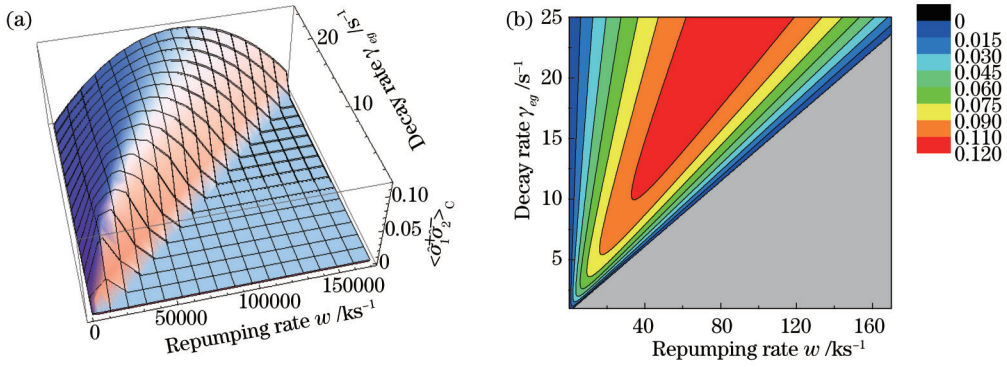

Fig.2 Spin-spin correlation with respect to the repumping rate and decay rate with a fixed atom number. (a) Three-dimensional graph; (b) contour map

condition becomes $w>\gamma$. At this threshold, the sign of the spin-spin correlation changes to positive, signifying the onset of the collective behavior, as shown in Fig. 2(a).

Interestingly, the sign of the spin-spin correlation changes again at a larger pump rate, above which the atoms return to normal non-collective emission. This upper threshold arises because $(w-\gamma)/(w+\gamma)$ eventually saturates at 1, while the pump induced noise grows with w. By setting $(w-\gamma)/(w+\gamma)=1$ and neglecting all atomic noise sources other than w, the maximum repumping rate is determined as $w_{\max}=N\gamma C$. Above this threshold, the pump noise destroys the coherence, as shown in Fig. 2(b). With larger spin-spin correlation, there is a stronger and more independent output, as well as a narrower linewidth. Eq. (2) allows us to determine the maximum spin-spin correlation of $\left\langle\hat{\sigma}_1^+\hat{\sigma}_2^-\right\rangle_C=1/8$, which is obtained at the repumping rate of $w_{\text{opt}}=N\gamma C/2$. At this pump rate, the laser power reaches its maximum of $P_{\max}=\hbar\omega N^2\gamma C/8$.

The ideal theoretical linewidth of a laser in this case can be given by a modified Schawlow-Townes fullwidth at half maximum (FWHM) equation[11]:

$$\Delta f_{\text{ST}}=hf(2\gamma_\perp\kappa)^2\Big/\left[4\pi P_{\text{out}}(2\gamma_\perp+\kappa)^2\right], \tag{3}$$

where P_{out} is the laser output power, f is the oscillation frequency, κ is the cavity power decay rate due to the mirror transmission alone, and h is the Planck constant. The transverse decoherence rate of the optical transition can be expressed as $\gamma_\perp=\gamma_{eg}/2+1/T_2$, where γ_{eg} is the single-particle decay rate from the upper state to the ground state, and $1/T_2$ is induced by other atomic dephasing mechanisms, such as spin dephasing.

If the cavity resonance frequency f_{cav}, and the atomic transition frequency f_{atomic} do not match, the system oscillates at a weighted frequency of

$$f=\left(2\gamma_\perp f_{\text{cav}}+\kappa f_{\text{atomic}}\right)\Big/\left(2\gamma_\perp+\kappa\right). \tag{4}$$

The cavity resonance frequency f_{cav} pulls the weighted frequency f from the atomic transition frequency by the level $P=f/f_{\text{cav}}=\gamma_\perp/(\gamma_\perp+\kappa)\approx\gamma_\perp/\kappa$, which is called the frequency-pulling coefficient. We determine the minimum atom number as $N=2/(T_2\gamma C)$. Below this critical number, $\left\langle\hat{\sigma}_1^+\hat{\sigma}_2^-\right\rangle_C$ is never positive, regardless of the strength of the repumping, and the collective dipoles are hence not constructed. The critical particle number can be estimated by Eq. (2). Physically, this equation indicates that there must be enough atoms for the system to enter the strong coupling regime. The red points shown in Figs. 3-6 represent the corresponding values in our theoretical model. The scaling of that power with the number of atoms indicates the collective nature of the emission shown in Fig. 3, suggesting that an output power of 7×10^{-10} W is possible in our theoretical model, with an atom number of N=10^6 (the red point).

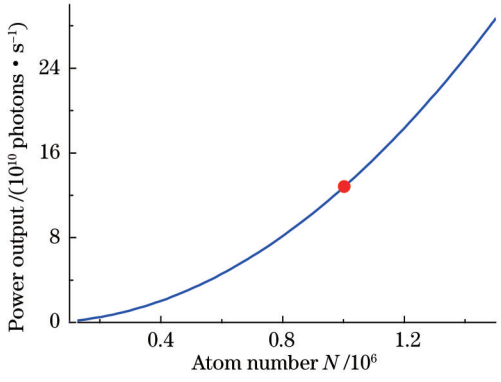

Fig.3 Output power with respect to atom number

As shown in Fig. 4(a), the cavity pulling coefficient P is around 4×10^{-5} for a range of γ_{eg} values. In the system, a group of ^{133}Cs atoms are confined to a low-finesse (F=300) optical cavity with a cavity power decay rate of $k=2\pi\times25$ MHz, $T_2\approx0.00032$ s. As the decay rate γ_{eg} decreases, the atomic dipole

becomes more isolated from the mirrors, as shown by the frequency-pulling coefficient P. In the bad cavity, the frequency-pulling coefficient is $P \approx 2\gamma_{\perp}/\kappa \ll 1$, drastically reducing the impact of the noise at the cavity frequency. This isolation of the oscillator from the environment is the key to abating the sensitivity of such a laser to thermal and technical noise. The output wavelength of the cesium bad-cavity laser system is pulled by the cavity resonance frequency (expressed in wavelength, ranging from 700 nm to 1100 nm), in Fig. 4(b) $2\gamma_{\perp}/\kappa$ =0.00004, 0.01, 0.1 respectively. Fig. 4(c) shows a close look at the change in weighted wavelength with $2\gamma_{\perp}/\kappa$ =0.00004.

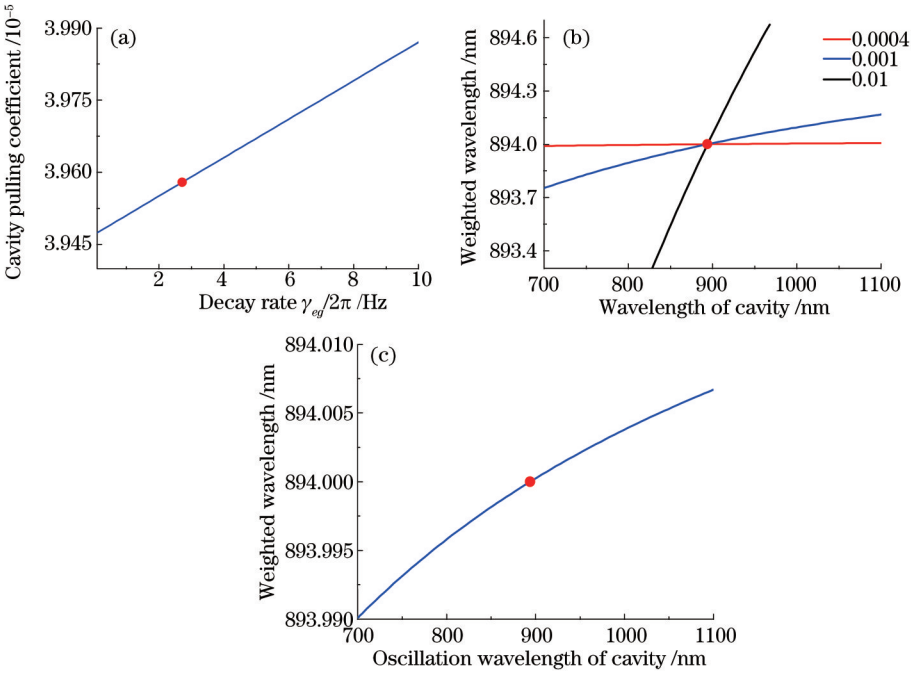

Fig.4 (a) Cavity pulling coefficient with respect to the decay rate; (b) relationship between the wavelength of the cesium bad-cavity laser system and the cavity resonance frequency; (c) change in the weighted wavelength

3 Results and analysis

In the optical bad cavity, with a limit of $2\gamma_{\perp} \ll \kappa$, the FWHM reduces to $\Delta f_{\mathrm{BST}} = \gamma_{\perp}^2/(\pi\kappa M_C)$, as shown in Fig. 5(a). With $2\gamma_{\perp}/\kappa$ from 1×10^{-5} to 1×10^{-3}, the excited-state scattering rate $\gamma_{eg} \approx 0.66-66\ \mathrm{s}^{-1}$, is comparable to those of atoms used in the optical clock, and the average intra-cavity photon number is $M_C = 20$. The linewidth of the system changes slightly with the cavity frequency according to the Schawlow-Townes equation with different values of $2\gamma_{\perp}/\kappa$, as shown in Fig. 5(b). The wavelength of the cesium bad-cavity laser system is pulled by the cavity resonance frequency.

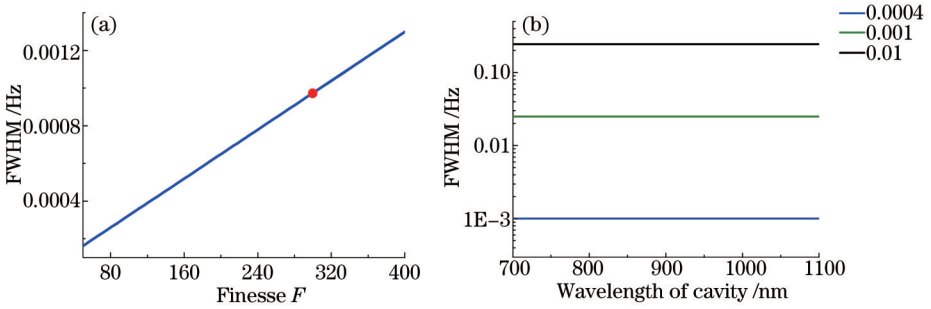

Fig.5 (a) Linewidth with respect to the finesse; (b) linewidth of the system changes slightly with the cavity frequency

To demonstrate the line shape of the power spectrum, we obtain the line-shape function using the following theory. The variable b^{+} is the photon-creation operator satisfying

$$b^{+}=\exp\left[\mathrm{i}\varphi\left(r_{0}+\rho\right)\right]\exp\left(\mathrm{i}\Omega t\right), \tag{5}$$

where φ is the phase shift due to noise, r_0 is a classical number, and ρ is the density matrix operator indicating the fluctuation of the amplitude. The output frequency is $\Omega=(\nu_{c}\chi+\gamma\omega)/(\chi+\gamma)$, where χ is the linewidth of the cavity, and ν_c is the cavity resonance frequency. The variables γ and ω are the self-decay linewidth and transition frequency of the atoms, respectively. Assuming that $\rho\ll r_0$ and $\exp(\mathrm{i}\Omega t)$ can be separated, Eq. (5) yields $b^{+}\approx r_{0}\exp[\mathrm{i}\varphi(t)]$. The correlation function is defined as $\left\langle b^{+}(t)b(0)\right\rangle$, and the φ_μ values are independent of each other, $\varphi(t)-\varphi(0)=\sum_{\mu}\varphi_{\mu}$.

$$b^{+}(t)b(0)\approx r_{0}^{2}\prod_{\mu}<\exp\left[-\mathrm{i}\varphi_{\mu}(t)\right]>\approx r_{0}^{2}\prod_{\mu}[1+\mathrm{i}\varphi_{\mu}(t)-\frac{1}{2}\varphi_{\mu}(t)^{2}]. \tag{6}$$

With $\left\langle\varphi_{\mu}\right\rangle=0$ and $\left\langle\varphi_{\mu}\varphi_{\mu'}\right\rangle=0\ (\varphi_{\mu}\neq\varphi_{\mu'})$, we obtain $\sum_{\mu}\varphi_{\mu}^{2}=\left[\varphi(t)-\varphi(0)\right]^{2}$. Combined with Eq. (5), we obtain

$$b^{+}(t)b(0)=r_{0}^{2}\exp\left\{-\left[\varphi(t)-\varphi(0)\right]^{2}/2\right\}. \tag{7}$$

Assuming $\Delta\omega=\frac{1}{2t}\left\langle\left[\varphi(t)-\varphi(0)\right]^{2}\right\rangle$ and $t>1/(\chi+\gamma)$, we obtain

$$\left\langle b^{+}(t)b(0)\right\rangle=r_{0}^{2}\exp(-\Delta\omega t). \tag{8}$$

By squaring and normalizing this, we obtain the line-shape function

$$g_{N}(\nu,\Omega)=2\Delta\omega/\left[\Delta\omega^{2}+4\pi^{2}(\nu-\Omega)^{2}\right], \tag{9}$$

where Ω is the center frequency of the oscillation, and the linewidth induced by the phase noise is $\Delta\omega/2\pi$. The linewidth deceases as the output power increases, which is the opposite case of the good cavity regime (green line), which is shown in Fig. 6(a). Compared with a rubidium laser, a cesium laser with the same output power has a narrower linewidth. Fig. 6(b) shows that an output power of 7×10^{-10} W is possible with a linewidth of 0.99 mHz without considering the light shift due to the dressing laser.

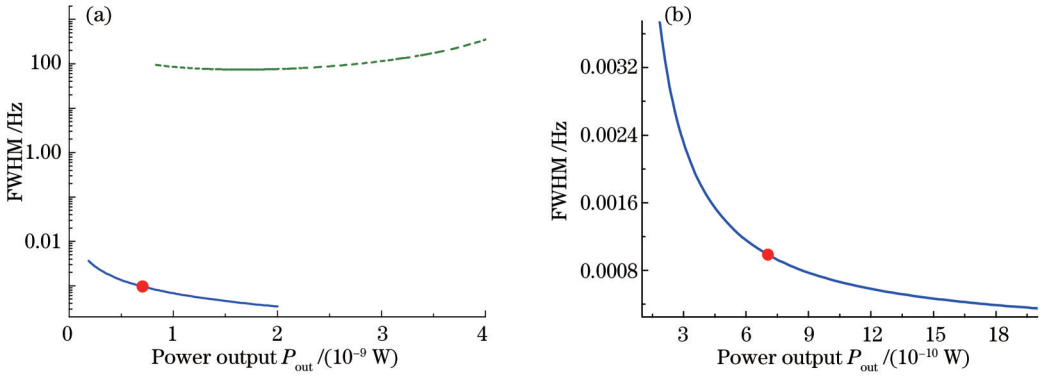

Fig.6 Relationship between laser linewidth and output power. (a) Comparison between a cesium bad-cavity laser (blue) and He-Ne laser in good-cavity regime (green); (b) cesium bad-cavity laser alone

Because of the narrow linewidth, the frequency standard can be applied. The layout for the new optical clock scheme is shown in Fig. 7. The repumping laser, at 852.3 nm, is constructed by an extended cavity laser diode resulting in a linewidth on the order of megahertz. The dressing laser, at 894.6 nm, is stabilized by an ultra-stable cavity, resulting in a linewidth of about 1 Hz. Both the lasers pass and couple with the ^{133}Cs atoms, which are trapped in the magic optical lattice. The two lasers are both constructed by an external cavity diode laser (ECDL), and the dressing laser is stabilized by an ultra-stable cavity. These two lasers interact with ^{133}Cs atoms trapped in the magic optical lattice at 852 nm. The bad-cavity laser emits photons into the optical bad-cavity regime, from which an optical frequency standard at 894.6 nm with a linewidth of about 1 mHz is output. In reference [16], the present linewidth

is limited by the atomic population noise. The first proposed active optical clocks[9,19] have been extended to different configurations[8,10-11,16,18,20-23], including the bad-cavity Raman laser configuration[16] with atoms trapped in the lattice and ^{133}Cs atoms trapped in the magic optical lattice at 852 nm[24-25]. Moreover, with a lower repumping light intensity and narrower repumping linewidth of about 100 Hz, we consider that it is possible for the bad-cavity Raman laser to emit photons into the optical bad-cavity regime with a theoretical linewidth less than 1 mHz[26-28].

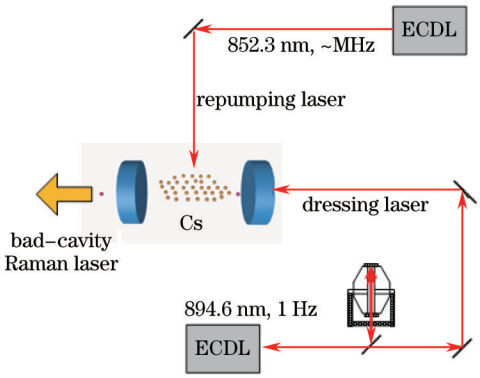

Fig.7 Experimental layout

4 Conclusions

We predict that the optical radiation in the bad-cavity configuration has an extremely narrow ideal theoretical linewidth in the 98×10^{-2} mHz range, without considering the light shift caused by the dressing laser, as well as a power level of 7×10^{-10} W, which is sufficient for phase locking a slave optical oscillator. We choose a cesium system for its long wavelength transition of cesium-133. The frequency pulling coefficient drastically reduces the impact of noise at the cavity frequency. This isolation of the oscillator from the environment is the key to reducing the sensitivity of such a laser to thermal and technical noise. Although the frequency pulling coefficient varies drastically, the linewidth of the oscillator can be impacted by its wavelength to some extent. Therefore, we examine all the alkali metal atoms, discovering that the transition probability of the atomic ground state to the first excited state for cesium is large and that the wavelength (894.6 nm) is longer than that of rubidium (795 nm). This means that the linewidth limit becomes smaller than that of rubidium-87 under the same conditions, and a bad-cavity laser in cesium-133 atomic dipoles theoretically has an extremely narrower quantum linewidth limit than the rubidium system. Moreover, to further reduce the frequency pulling coefficient, we design the optical bad-cavity regime with a lower finesse, and the linewidth is narrower.

For more power, we propose a system with more atoms, and an average of 20 photons inside the optical cavity are maintained. This guarantees a power level of 7×10^{-10} W, which is important for practical applications. The mechanism of the active optical clock operating in the bad-cavity configuration can potentially provide a new method for realizing an optical clock with a millihertz linewidth, which makes atomic clocks more stable, as the millihertz linewidth is far beyond the present coherence time realized by passive optical clocks.

References

1 Chou C W, Hume D B, Koelemeij J C J, *et al.*. Frequency comparison of two high-accuracy Al^+ optical clocks[J]. Phys Rev Lett, 2010, 104: 070802.

2 Tamm C, Weyers S, Lipphardt B, *et al.*. Stray-field-induced quadrupole shift and absolute frequency of the 688 THz $171Yb^+$ single-ion optical frequency standard[J]. Phys Rev A, 2009, 80: 043403.

3 Birnbaum K M, Boca A, Miller R, *et al.*. Photon blockade in an optical cavity with one trapped atom[J]. Nature, 2005, 436:

87-90.

4 Marshall W, Simon C, Penrose R, *et al.*. Towards quantum superpositions of a mirror[J]. Phys Rev Lett, 2003, 91: 130401.

5 Müller H, Herrmann S, Braxmaier C, *et al.*. Modern Michelson-Morley experiment using cryogenic optical resonators[J]. Phys Rev Lett, 2003, 91: 020401.

6 Jiang Y Y, Ludlow A D, Lemke N D, *et al.*. Making optical atomic clocks more stable with 10-16 level laser stabilization[J]. Nature Photon, 2011, 5: 158-161.

7 Young B C, Cruz F C, Itano W M, *et al.*. Visible lasers with subhertz linewidths[J]. Phys Rev Lett, 1999, 82: 3799-3802.

8 Meiser D, Ye J, Carlson D R, *et al.*. Prospects for a millihertz-linewidth laser[J]. Phys Rev Lett, 2009, 102: 163601.

9 Chen J B. Active optical clock[J]. Chin Sci Bull, 2009, 54(3): 348-352.

10 Wang Y Q. Optical clocks based on stimulated emission radiation[J]. Chin Sci Bull, 2009, 54(3): 347.

11 Yu D S, Chen J B. Laser theory with finite atom-field time[J]. Phys Rev A, 2008, 78: 013846.

12 Bassani F, Forney J J, Quattropani A. Choice of gauge in two-photon transitions: 1s-2s transition in atomic hydrogen[J]. Phys Rev Lett, 1977, 39(17): 1070-1073.

13 Hemmerich A, Hänsch T W. Two-dimensional atomic crystal bound by light[J]. Phys Rev Lett, 1993, 70: 410-413.

14 Dicke R H. Coherence in spontaneous radiation processes[J]. Phys Rev, 1954, 93(1): 99-110.

15 Haake F, Kolobov M I, Fabre C, *et al.*. Superradiant laser[J]. Phys Rev Lett, 1993, 71(7): 995-998.

16 Bohnet J G, Chen Z L, Weiner J M, *et al.*. A steady-state superradiant laser with less than one intracavity photon[J]. Nature, 2012, 484: 78-81.

17 Wang Y F, Chen J B. Superradiant laser with ultra-narrow linewidth based on ^{40}Ca[J]. Chin Phys Lett, 2012, 29(7): 073202.

18 Meiser D, Holland M J. Steady-state superradiance with alkaline-earth-metal atoms[J]. Phys Rev A, 2010, 81: 033847.

19 Chen J B, Chen X Z. Optical lattice laser[C]. Proceedings of 2005 IEEE International Frequency Control Symposium, 2005: 608-610.

20 Zang X, Zhang T, Chen J. Magic wavelengths for a lattice trapped rubidium four-level active optical clock[J]. Chin Phys Lett, 2012, 29: 090601.

21 Zhang T, Wang Y, Zang X, *et al.*. Active optical clock based on four-level quantum system[J]. Chin Sci Bull, 2013, 58: 2033-2038.

22 Zhang S N, Wang Y F, Wang D Y, *et al.*. A scheme of potassium atom four level active optical clock[J]. Chin Phys Lett, 2013, 30: 040601.

23 Kazakov G A, Schumm T. Active optical frequency standard using sequential coupling of atomic ensembles[J]. Phys Rev A, 2013, 87: 013821.

24 Chalupczak W, Szymaniec K, Henderson D. Cooling in an optical lattice for a caesium fountain frequency standard[J]. IEEE Trans Instrum Meas, 2005, 54(2): 837-841.

25 Dion C M, Sjolund P, Petra S J H, *et al.*. Time dependence of laser cooling in optical lattices[J]. Europhys Lett, 2005, 72(3): 369-375.

26 Shen Yanlong, Chen Hongwei, Huang Ke, *et al.*. Watt-level 100-nm tunable mid-infrared Er∶ZBLAN fiber laser[J]. Chinese J Lasers, 2015, 42(10): 1002008.
沈炎龙, 谌鸿伟, 黄 珂, 等. 瓦级100-nm可调谐中红外Er:ZBLAN光纤激光器[J]. 中国激光, 2015, 42(10): 1002008.

27 Wu Yongzhong, Zhu Jianqiang, Li Yangshuai. Design of non-imaging pump cavity of laser rod amplifier[J]. Chinese J Lasers, 2015, 42(10): 1002007.
吴永忠, 朱健强, 李养帅. 激光棒状放大器非成像抽运腔设计[J]. 中国激光, 2015, 42(10): 1002007.

28 Jin Dongchen, Sun Ruoyu, Wei Shouyu, *et al.*. 1570 nm nanosecond pulse generation from Er/Yb co-doped all-fiber dual-cavity laser with fiber-based passive *Q*-switched[J]. Chinese J Lasers, 2015, 42(10): 1002006.
金东臣, 孙若愚, 魏守宇, 等. 基于光纤被动调*Q*的1570 nm纳秒脉冲铒镱双掺全光纤双腔激光器[J]. 中国激光, 2015, 42(10): 1002006.

栏目编辑：史 敏